showed unequivocally that for $p \geq 4$, there is a constant C_p such that if $\delta > \varepsilon A^p C_p$, then the solution emanating from initial data u_0 of amplitude A exists globally in time and decays to the mean of u_0 exponentially. This sharp agreement between analytically and numerically deduced information regarding a supposed scaling law for δ_c lends credence to its existence. Analogous numerical experiments for the zero$^{\text{th}}$-order dissipative problem (2.14) confirm the validity of a scaling law of the form (2.23) for σ_c.

With this background discussion and preview of some of the more important conclusions in hand, attention is now directed to a detailed description of the outcome of our numerical experiments. Reported first are computations for the initial- and periodic-boundary-value problem (1.3) with $p = 5, 6$ and 7. The borderline case $p = 4$ had already proved to be more difficult to understand when $\delta = 0$, and so it was not included in the present study. We first consider, as in the previous study, initial data which is a simple amplitude perturbation of a solitary-wave, to wit

$$u_0(x) = \lambda A \operatorname{sech}^{2/p}(K(x - \tfrac{1}{2})) \tag{4.3}$$

with K as in (2.12b) and with the perturbation parameter $\lambda > 1$ typically taken to be 1.01.

Consider the case with $A = 2.0$, $\lambda = 1.01$, $p = 5$ and $\varepsilon = 5 \times 10^{-4}$ which was studied with $\delta = 0$ in Bona *et al.* (1994). As seen clearly in Figure 6 of the last-quoted reference, the solitary wave rapidly lost it shape and its peak became unbounded, whilst exhibiting self-similar behavior. Let $M(t)$ be some norm of the solution emanating from (4.3), say, that becomes infinite in finite time. Its rate of blow-up is ρ where $M(t) \sim (t^* - t)^{-\rho}$ as $t \to t^*$, where t_* is as before, the blow-up time. The rate ρ is approximately equal to

$$\rho = \frac{-\log[M(\tau_1)/M(\tau_2)]}{\log[(\tau^* - \tau_1)/(\tau^* - \tau_2)]},$$

where τ_1, τ_2 are two distinct instances of $t < t^*$, but near t^*, where $M(t)$ is known.

The blow-up rates were computed for the approximate solution for the L_q-norms with $q = p-1,\ p,\ p+1,\ p+2,\ \infty$ and for the L_2- and L_∞-norms of its spatial derivative (denoted

$L_{2,D}$ and $L_{\infty,D}$, respectively). Naturally, the blow-up rates will not usually settle down to their asymptotic values until t is quite close to t^*. In Table 1 below are reproduced the numerically computed blow-up rates corresponding to the approximate solution emanating from the just-mentioned perturbed solitary wave at the times τ_i at which the computer code calls for the i^{th} spatial refinement. For details, the reader may consult Section 5 of Bona *et al.* (1994).

i	L_{p-1}	L_p	L_{p+1}	L_{p+2}	L_∞	$L_{2,D}$	$L_{\infty,D}$
5	.5029(-1)	.6683(-1)	.7795(-1)	.8590(-1)	.1336	.3008	.4657
10	.5047(-1)	.6729(-1)	.7853(-1)	.8657(-1)	.1348	.3028	.4731
15	.4983(-1)	.6647(-1)	.7759(-1)	.8554(-1)	.1334	.2992	.4618
20	.4989(-1)	.6658(-1)	.7773(-1)	.8572(-1)	.1338	.2999	.4690
25	.5044(-1)	.6728(-1)	.7851(-1)	.8654(-1)	.1347	.3029	.4747
30	.4974(-1)	.6633(-1)	.7741(-1)	.8534(-1)	.1329	.2985	.4685
35	.5001(-1)	.6672(-1)	.7786(-1)	.8583(-1)	.1336	.3004	.4654

Table 1

Blow-up rates. Perturbed Solitary wave, $p = 5$, $\varepsilon = 5 \times 10^{-4}$, $\delta = 0$,
$\tau_f = .22549 \times 10^{-1}$, $f = 42$, $x^* = .61333$, $U_{\max} = 224,766$,
$k_{\min} = .23 \times 10^{-40}$, $\Delta\tau_f = .16 \times 10^{-38}$.

The tolerance levels used to trigger the spatial and temporal refinements in the result represented in Table 1 were chosen on the basis of extensive computational experience. Simulations to be reported presently of the dissipative case utilized the same values of these parameters. In the legend of Table 1 are recorded the final time τ_f that is achieved after f spatial refinements, the approximate point $x^* \in [0,1]$ of blow-up and the amplitude $U_{\max}$ that the numerical approximation attained at $t = \tau_f$. The parameter $k_{\min}$ is the smallest time step arising in the computations and $\Delta\tau_f$ is the temporal increment the program made between the last two spatial refinements. Initially, the spatial meshlength was $h_0 = 1/192$ and the time step $k_0 = 10^{-3}$. It is useful to compare the blow-up rates in Table 1 to those that would obtain if the solution had the form depicted in (4.2). For

the reader's convenience, these hypothetical rates for the case $p = 5$ are displayed in Table 2. The agreement between corresponding values in Tables 1 and 2 lends credibility to the conjecture in (4.2). Graphs of the solution as a function of x for various values of t provided in Bona *et al.* (1994) also support the conclusion that the putative blow-up has a similarity form.

Norm	L_4	L_5	L_6	L_7	L_∞	$L_{2,D}$	$L_{\infty,D}$
Rate	.500(-1)	.667(-1)	.778(-1)	.857(-1)	.133	.300	.467

Table 2

Predicted blow-up rates according to (4.2) for $p = 5$.

What happens to the picture just outlined when dissipation is added? To approach this issue, we considered the approximation of a solution of (1.3) with all the parameters for the initial data as in the simulation just described except that δ was set to the positive value 2×10^{-4}. The parameters relating to the numerical scheme are also as above except that the initial time step k_0 was taken to be 1/1600 to minimize the numerical errors associated with the first stage of the integration.

The evolution in time of the approximate solution in the case of positive dissipation is depicted in the sequence of plots in Figure 1. The first four plots, which comprise Figure 1a, show the same response to the perturbation that was observed in the dissipationless case, namely the formation of a thin spike which proceeds to blow up at about the point $(x^*, t^*) = (.65812, .038624)$. In the graphs displayed in Figure 1a, the solution appears to blow up at $x_0 = 1/2$, but this is due to the occasional translations of the peak back to $x = 1/2$ to keep the maximum value of the solution located in the interval with the finest grid. This strategy allowed us to refine the spatial grid in a static way rather than moving the grid to follow the peak. (Actually, our simulations suggest that the center $X(t)$ of the peak at time t behaves according to the law $X(t) \sim x^* + C(t^* - t)^{1/3}$ as t approaches t^*, where C is some negative constant depending on δ, ε, p and u_0.) The second set of four

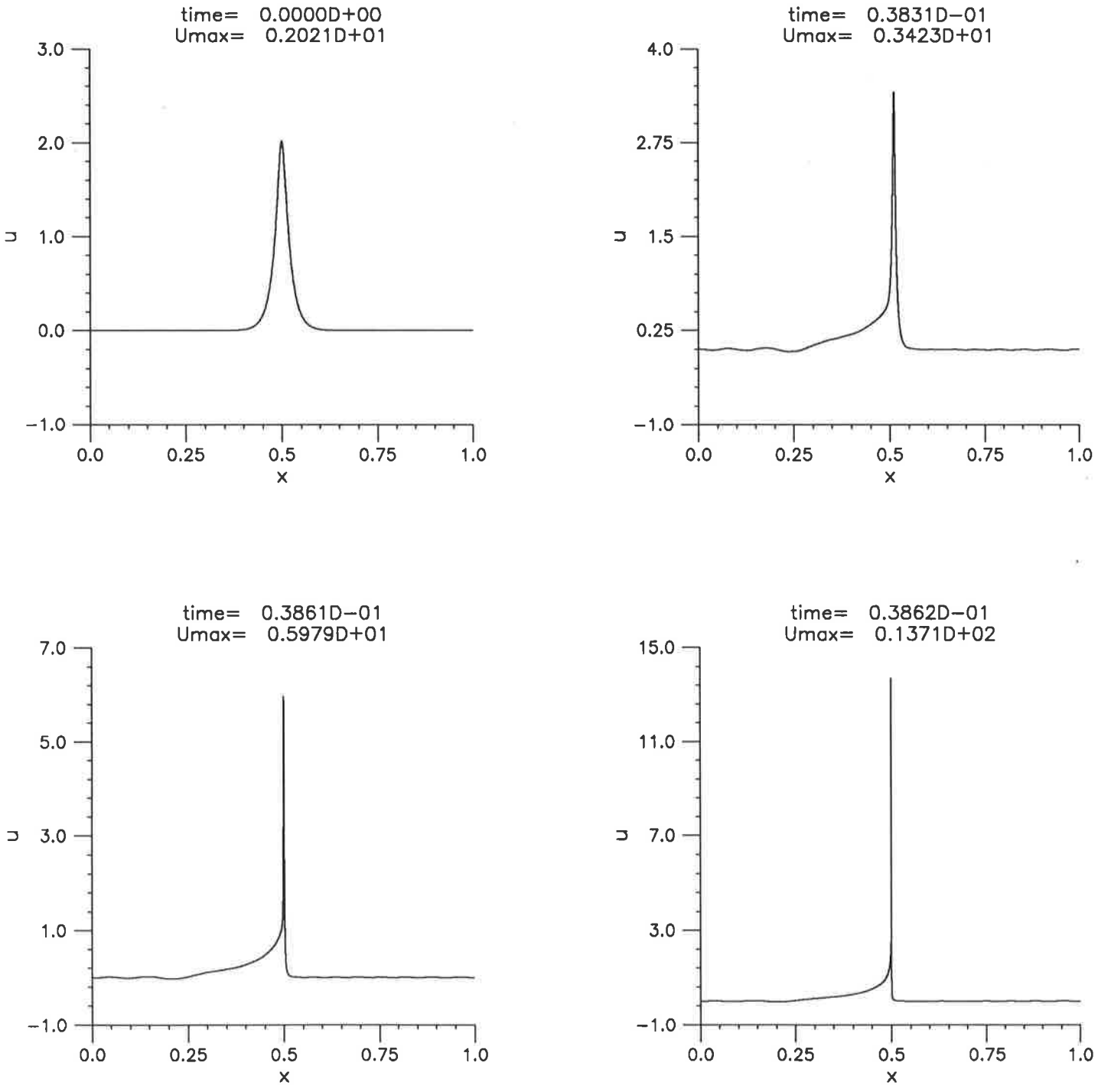

Figure 1a

Blow-up in the presence of small dissipation.

Perturbed solitary wave, $p = 5,\ A = 2,\ \lambda = 1.01,\ \varepsilon = 5 \times 10^{-4},\ \delta = 2 \times 10^{-4}$.

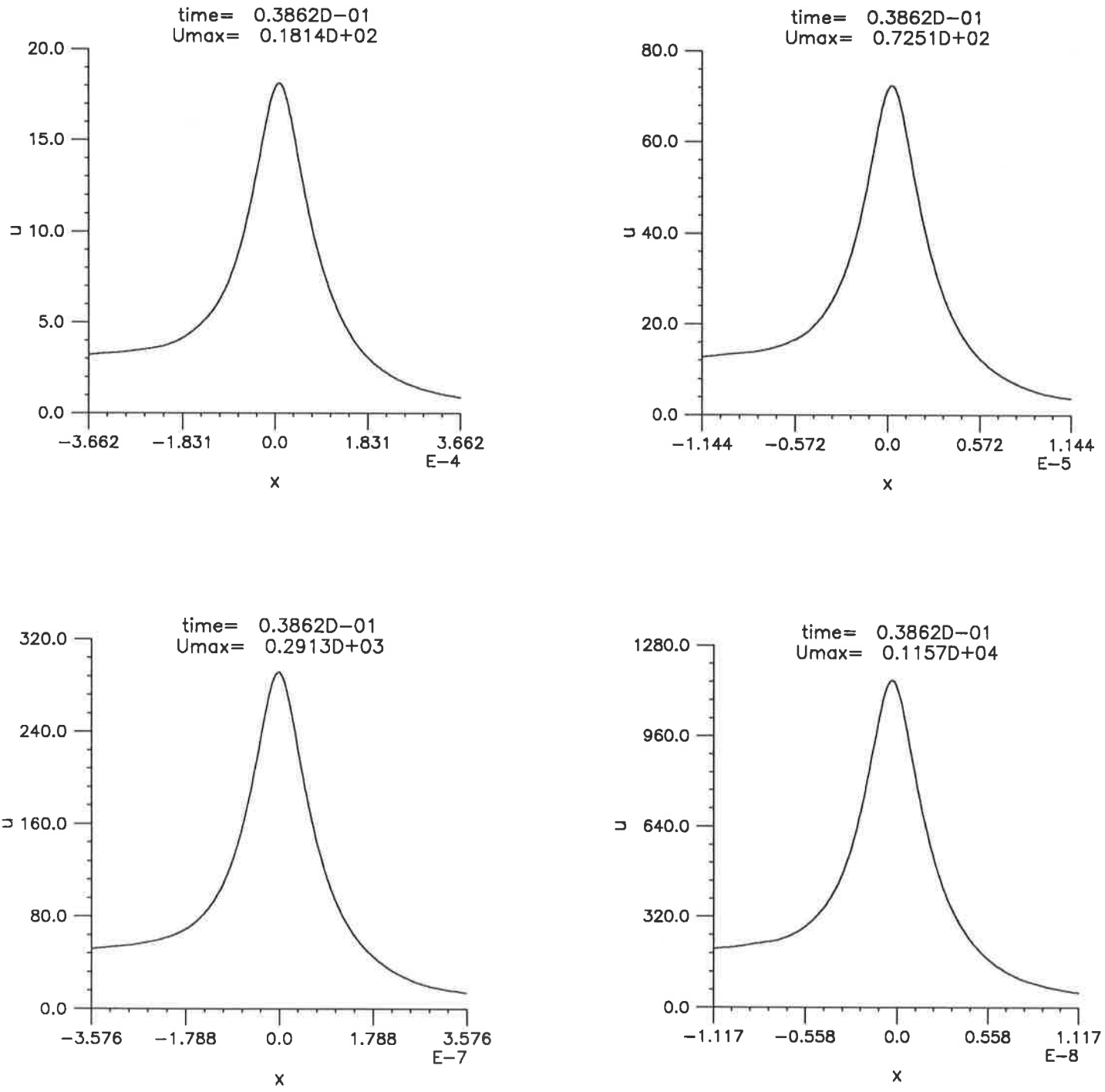

Figure 1b
Self-similarity of the blow-up. Data taken from the run of Figure 1a.

graphs in Figure 1b show, on a suitably rescaled set of x-t axes, a detailed view of the peak as it blows up. In these graphs the peak has been relocated to about $x = 0$ and the depiction is only that portion of the solution in the interval corresponding to the finest spatial grid (e.g. $[-6.81 \times 10^{-13},\ 6.81 \times 10^{-13}]$ in the fourth plot). These plots make plausible the presumption that there is a similarity structure through which the blow-up proceeds. Having determined that the solution corresponding to $\delta = 2 \times 10^{-4}$ and the previously mentioned perturbed solitary-wave initial data appears to form a singularity at a finite time t^*, it seemed appropriate to compute its blow-up rates near t^*. These are shown in Table 3, whose legend provides the precise values of all the parameters pertaining to this simulation. As in Table 1, there appears to be well-defined asymptotic blow-up rates associated with this solution, and, moreover, these blow-up rates are sensibly the same as those in Tables 1 and 2. Similar agreement in blow-up rates was observed in the analogous numerical experiments with perturbed solitary waves for $p = 6$ and 7. We also performed a set of experiments with initial data

$$u_0(x) = A\, e^{-100(x-\frac{1}{2})^2}, \tag{4.4}$$

which is a Gaussian profile not specifically tied to a travelling-wave solution of (1.1a). When an approximate solution was developed using our scheme and $A = 1$, $p = 5$, $\varepsilon = 2 \times 10^{-4}$ and $\delta = 10^{-4}$, it was found that the solution apparently blew up in finite time, at about the point $(x^*, t^*) = (.72886,\ .37376)$ where the approximate solution U had attained a value $U_{\max} = 17,148$. The form of the blow-up was much like that observed in the non-dissipative case (see §5 of Bona *et al.* 1994). In addition, the blow-up rates of the various norms of the solution emanating from the u_0 in (4.4) all agree to at least two digits with those for the solitary wave shown in Table 3. This lends further support to a scenario that is described as follows. The Gaussian initial data quickly resolves into a solution dominated by pulses that resemble solitary waves. The largest of these then becomes unstable and proceeds to form a singularity in finite time through the same route as seen already for the perturbed solitary wave in Figure 1.

i	L_{p-1}	L_p	L_{p+1}	L_{p+2}	L_∞	$L_{2,D}$	$L_{\infty,D}$
5	.5049(-1)	.6700(-1)	.7814(-1)	.8612(-1)	.1341	.3009	.4639
10	.4995(-1)	.6655(-1)	.7763(-1)	.8555(-1)	.1331	.2994	.4594
15	.5000(-1)	.6670(-1)	.7787(-1)	.8586(-1)	.1339	.3004	.4660
20	.4987(-1)	.6645(-1)	.7747(-1)	.8533(-1)	.1325	.2988	.4598
25	.5012(-1)	.6688(-1)	.7808(-1)	.8609(-1)	.1343	.3012	.4683
30	.5012(-1)	.6681(-1)	.7793(-1)	.8587(-1)	.1334	.3006	.4720
35	.5007(-1)	.6675(-1)	.7786(-1)	.8579(-1)	.1333	.3003	.4665

Table 3

Blow-up rates. Perturbed solitary wave initial data, $p = 5$, $\varepsilon = 5 \times 10^{-4}$, $\delta = 2 \times 10^{-4}$
$\tau_f = .38624 \times 10^{-1}$, $f = 39$, $x^* = .65812$, $U_{\max} = 98,050$, $k_{\min} = .60 \times 10^{-38}$,
$\Delta\tau_f = .77 \times 10^{-36}$.

It appears that the major effect of a small amount of dissipation added to the nonlinear, dispersive equation (1.1) is just to delay the blow-up. This is seen by comparing the approximate blow-up times τ_f in Tables 1 and 3. Since the peak propagates in the direction of increasing values of x, the blow-up point x^* is consequently translated to the right as well.

This paradigm changes as the level of dissipation increases. For example, repeating the numerical experiment corresponding to Figure 1, except with δ increased to 10^{-3}, the approximate solution was soon observed to develop dispersive oscillations followed by a steady decrease in the maximum amplitude (see Figure 2). By the time t had the value .09974, the largest excursion of the approximate solution was only about 1.03. A more detailed view of the temporal decay of this solution will be provided in the next subsection.

This pair of experiments pointed to the following possibility: For fixed initial data u_0 that leads to the formation of a singularity in finite time when $\delta = 0$, there is a critical value δ_c of δ such that solutions emanating from u_0 will form a singularity in finite time if $\delta < \delta_c$, and will exist globally in time if $\delta > \delta_c$.

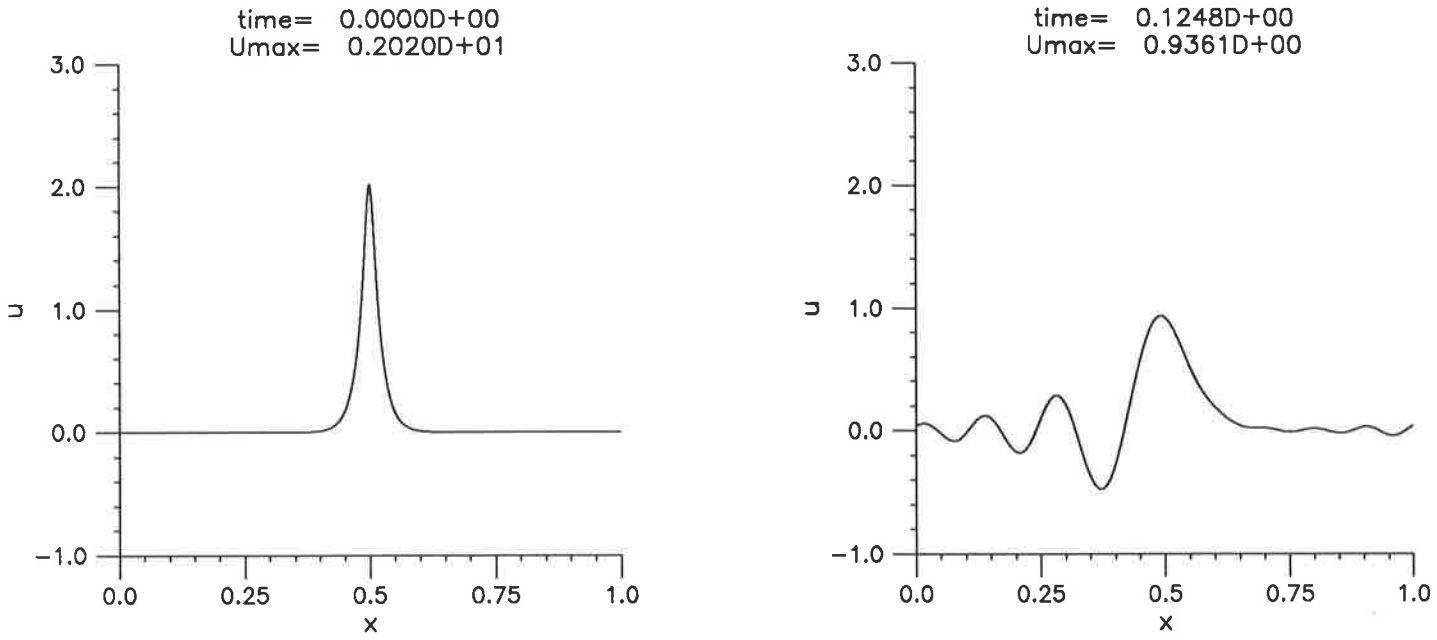

Figure 2

Oscillations and decay in the presence of larger dissipation.

Perturbed solitary wave, $p = 5,\ A = 2,\ \lambda = 1.01,\ \varepsilon = 5 \times 10^{-4},\ \delta = 10^{-3}$.

This hypothesis was copiously tested by several sequences of numerical experiments with perturbed solitary waves of the form (4.3) as initial data. Some of these results were presented in detail in Section 4 of Bona *et al.* (1992). On the basis of such experiments, a conjecture was stated in the just cited reference to the effect that there is a critical value c_p, depending only on p, of the parameter $\Delta = \delta^2\varepsilon/A^p$, such that if $\Delta < c_p$ the solution blows up at a point in finite time, while if $\Delta > c_p$, the solution exists for all t. The second part of this conjecture has now been proved (cf. Theorem 2.1 and subsequent remarks in Section 2; the constant C_p in (2.13) can be traced through the proof and, not surprisingly, turns out to be much larger than the experimentally observed value c_p.)

For a perturbed solitary-wave initial datum of the type (4.3) and a given set of parameters A, ε, p and λ (as mentioned before, we always took $\lambda = 1.01$ and experimented with $p = 5, 6$ and 7), we recorded two nearby values δ_c^- and δ_c^+ of the dissipation parameter, selected so that there was definite blow-up if $\delta \leq \delta_c^-$ and definite global existence and decay if $\delta \geq \delta_c^+$. As an example, we show the outcome of one such experiment corresponding to $p = 5,\ A = 2,\ \lambda = 1.01$, giving δ_c^- and δ_c^+ for various values of ε:

ε	δ_c^-	δ_c^+
.10(−3)	.10(−3)	.11(−3)
.25(−3)	.16(−3)	.17(−3)
.50(−3)	.230(−3)	.235(−3)
.80(−3)	.28(−3)	.30(−3)

The transition between 'definite' decay and 'definite' blow-up was quite sharp. This enabled us to define with some confidence a computationally determined version of the critical value δ_c to be the average of the sharpest achieved values δ_c^- and δ_c^+ after making the interval (δ_c^-, δ_c^+) as narrow as was computationally convenient.

In Table 4 we show, for $p = 5, 6$ and 7 and for various values of the amplitude A, the value of the parameter δ_c^2/ε. (This was computationally checked to be independent of ε for fixed A, p and λ; the particular data of Table 4 correspond to $\varepsilon = 5 \times 10^{-4}$). We also record the numbers $c_p = \delta_c^2/\varepsilon A^p$. The data clearly suggest that c_p is independent of A

and seems to be an increasing function of p, equal to about $.34 \times 10^{-5}$, 1.22×10^{-5}, and 2.42×10^{-5} for $p = 5, 6$ and 7, respectively.

A	$p = 5$		$p = 6$		$p = 7$	
	δ_c^2/ε	c_p	δ_c^2/ε	c_p	δ_c^2/ε	c_p
1.5	.026(-3)	.3483(-5)	.140(-3)	1.2330(-5)	.414(-3)	2.4233(-5)
2	.108(-3)	.3379(-5)	.781(-3)	1.2207(-5)	3.100(-3)	2.4219(-5)
2.5	.328(-3)	.3359(-5)	2.952(-3)	1.2093(-5)	1.485(-2)	2.4332(-5)
3	.832(-3)	.3424(-5)	8.862(-3)	1.2156(-5)	5.315(-2)	2.4302(-5)

Table 4
Critical values δ_c^2/ε and $c_p = \delta_c^2/\varepsilon A^p$
for blow-up of perturbed solitary wave initial value (4.3), $\lambda = 1.01$.

As discussed already, other classes of initial conditions resolve themselves into solitary waves plus a dispersive tail, even in the presence of dissipation. One would expect that if the largest solitary wave that emerges has amplitude A, then for δ large enough to guarantee the decay of this solitary wave, there should exist a global solution evolving from the given initial condition. On the other hand, if δ is such that the corresponding Δ is below its critical value, then it is expected that the solution will blow up in finite time.

We close this subsection with a brief computational study of the effect of the zero$^{\text{th}}$ order dissipation term σu on the behavior of solutions of the initial value problem (2.14) evolving from perturbed solitary-wave initial data of the form (4.3). As remarked in Section 2, if $\Sigma = (\sigma^2\varepsilon)^{1/3}/A^p$ is sufficiently large, a global solution exists, in fact decaying to zero in L_2 exponentially as $t \to \infty$. The numerical experiments conform to this fact and indicate that there exists a constant c_p', depending only on p, such that if $\Sigma < c_p'$ the solution blows up in finite time, whereas if $\Sigma > c_p'$ it will exist globally. In the event of blow-up, the blow-up rates were almost identical to the ones observed in the case of the (undamped) problem (1.1), suggesting that a similarity structure of the type (4.2) is formed again. Thus, the self-similar profile given by (4.2) proves to be quite stable under both types of dissipation

considered here. It should be noted that (2.14) seems to be a harder problem to integrate numerically up to blow-up as compared with (1.3), the reason probably being that as the blow-up is delayed by dissipation, small numerical oscillations may pollute somewhat the solution as it blows up. Such oscillations are likely to be damped more effectively by the second-order term $-\delta u_{xx}$.

Table 5 shows the results of a series of typical numerical experiments for $p = 5$ and various values of A, σ and ε. (We took $\lambda = 1.01$ as usual.) For a given value of A and σ, we varied ε and recorded a pair of nearby values ε_+ and ε_- chosen so that the interval $[\varepsilon_-, \varepsilon_+]$ was narrow, with definite blow-up as the outcome if $\varepsilon = \varepsilon_-$ and with definite global existence and decay if $\varepsilon = \varepsilon_+$. For the blow-up value, we also record $U_{\max}$ the maximum amplitude reached at the end of the computation, as well as τ_f, the approximate blow-up time. The critical value is indeed seen to be a constant, equal to about 1.8×10^{-3} independently of A, σ and ε.

A	σ	ε	Result	$U_{\max}$	τ_f	c'_p
1.7	.4	.11(-3)	decay			
		.10(-3)	blow-up	2071	.0776	1.804(-3)
1.8	.3	.44(-3)	decay			
		.43(-3)	blow-up	451	.1188	1.797(-3)
1.8	.4	.25(-3)	decay			
		.24(-3)	blow-up	2430	.0844	1.798(-3)
1.8	.5	.16(-3)	decay			
		.15(-3)	blow-up	1951	.0607	1.791(-3)
1.9	.4	.56(-3)	decay			
		.55(-3)	blow-up	107	.1030	1.802(-3)

Table 5

Blow-up and decay of (2.14). Perturbed solitary wave initial data, $\lambda = 1.01$, $p = 5$.

The computed critical value of $\Sigma = (\sigma^2 \varepsilon_c)^{1/3}/A^p$ is given in the last column of the Table. (The value ε_c was taken as the average of the two recorded values ε_+ and ε_- of ε.)

4B. DECAY OF SOLUTIONS

In this section attention is restricted to the periodic initial-value problem (1.3) for the generalized Korteweg-de Vries-Burgers equation in which the spatial period of the initial data and the corresponding solution is normalized to be $L = 1$. The dissipation parameter δ is taken large enough that the problem has a global solution. In this case, it follows from Corollary 2.3, that the solution of (1.3) decays in L^2 exponentially fast, indeed, satisfying

$$|u(\cdot,t) - \overline{u}_0|_2 \leq e^{-(2\pi)^2\delta t}|u_0 - \overline{u}_0|_2, \tag{4.5}$$

where $\overline{u}_0 = \int_0^1 u_0(x)dx$. In addition, if u_0 belongs to $H^s(0,1)$, and satisfies the smallness condition (2.9) relative to δ, then all seminorms $|\partial_x^j u|_2$, $1 \leq j \leq s$, decay exponentially to zero as t grows. (In Corollary 2.3 the proof given yields that $|u_x(\cdot,t)|_2$ decays with a rate of $O(e^{-(2\pi)^2\delta' t})$ for some constant δ' with $0 < \delta' < \delta$.)

As may already be gleaned from the example presented in the previous subsection (cf. Figure 2), the solution evolving from, say, a solitary-wave initial profile, breaks up, develops an oscillatory tail that travels around due to periodicity and interacts with the bulk of the wave, thereby producing an irregular pattern of oscillations. As t grows, the various modes of the solution decay, with the highest ones vanishing first. Eventually, the solution settles down to a sinusoidal profile which decays to the constant $\overline{u}_0$ while travelling with a speed determined by $\overline{u}_0$ and the dispersive term in (1.3). Thus, for very large values of t, the solution is essentially governed by the linearized equation corresponding to (1.2).

In the first part of this section we shall study, by means of numerical experiments, the details of the just outlined behavior of the long-time decay of solutions. In the second part we shall present numerical examples illustrating the short-time oscillatory break-up of solutions and provide a brief commentary on this phenomenon.

Biler (1984), using techniques of Foias and Saut (1984), has proved sharp decay estimates as $t \to \infty$ for the solutions of a class of nonlinear dispersive equations with dissipation, posed on an interval with periodic boundary conditions. His theory covers the initial-

and periodic-boundary-value problem (1.3) for $\overline{u}_0 = 0$ and $p < 2$, and shows, essentially, that $\lim_{t\to\infty} \frac{\log|u(t)|_2}{t} = \lim_{t\to\infty} \frac{\log|u_x(t)|_2}{t} = -\delta\Lambda$ where Λ depends on u_0 and is one of the eigenvalues $(2\pi n)^2$, $n = 1, 2\ldots$, of the operator $-\frac{d^2}{dx^2}$ on $[0,1]$ (i.e. of the differential operator in the dissipative term), with periodic boundary conditions at the endpoints. Hence, both $|u|_2$ and $|u_x|_2$ are $O(e^{-\delta\Lambda t})$ as $t \to \infty$. Here, for two types of initial conditions u_0, and for $p = 5$ and 6, we shall present computational evidence which, among other things, suggests that in various norms the solution of (1.3) decays to $\overline{u}_0$ in such a way that it is $O(e^{-(2\pi)^2\delta t})$ as $t \to +\infty$. In particular, the decay rate in (4.5) appears to be sharp.

In a first experiment, we took $p = 5$, $\varepsilon = 0.5 \times 10^{-3}$, $\delta = 0.2 \times 10^{-3}$, and, as initial value, the perturbed solitary wave of the form (4.3) with $A = 1.5$, $\lambda = 1.01$, and mass $\overline{u}_0 = .141258$. For all norms or seminorms $M(\cdot)$ (see below) considered, it was observed that the decay was indeed exponential We then determined for each quantity M the constants B and μ such that

$$M(u(t) - \overline{u}_0) \simeq Be^{-\mu t}, \quad \text{as} \quad t \to \infty. \tag{4.8}$$

This was accomplished by computing $M_i = M(u(t_i) - \overline{u}_0)$ at times $t_i = t_0 + i\Delta t$, $i = 1, 2, \ldots$, where $\Delta t = 2$, and determining for each i the values

$$\mu_i = \frac{-1}{\Delta t} \log\left(\frac{M_i}{M_{i-1}}\right).$$

and

$$B_i = M_i \exp\,(\mu_i t_i)$$

The results are shown in Table 6 for t up to 500. The quantities $M(v)$ are the norms $|v|_q, q = 2, p, \infty$, and also, the seminorms $|v_x|_2$ and $|v_x|_\infty$. For each M and different values of t_i, the corresponding computed values of μ_i and B_i are recorded in Table 6a and Table 6b, respectively. We also show the rates and constants for the $|v|_q$ norms for $q = p - 1$, $p + 1$ and $p + 2$ only at the final instance $t = 500$ since their evolution with increasing t closely resembles that of the entries of the L^p column.

t	L_2	L_p	L_∞	$L_{2,D}$	$L_{\infty,D}$
20	.15061(-1)	.49132(-1)	.10203	.37086(-1)	.18847
40	.10434(-1)	.14300(-1)	.15728(-1)	.16468(-1)	.48906(-1)
60	.89678(-2)	.53166(-2)	-.33487(-1)	.99156(-2)	.36859(-1)
80	.83190(-2)	.10563(-1)	.41326(-1)	.10284(-1)	-.18133(-1)
100	.80498(-2)	.86300(-2)	.19954(-1)	.84097(-2)	-.62585(-2)
200	.78970(-2)	.78983(-2)	.49293(-2)	.79085(-2)	.14790(-1)
300	.78957(-2)	.78961(-2)	.83062(-2)	.78961(-2)	.76502(-2)
400	.78957(-2)	.78957(-2)	.79115(-2)	.78957(-2)	.78744(-2)
500	.78957(-2)	.78957(-2)	.78934(-2)	.78957(-2)	.79025(-2)

t	L_{p-1}	L_{p+1}	L_{p+2}
500	.78957(-2)	.78957(-2)	.78957(-2)

Table 6a

Decay parameters μ. Perturbed solitary-wave initial profile, $p = 5, \delta = 0.2 \times 10^{-3}, \varepsilon = 0.5 \times 10^{-3}$.

t	L_2	L_p	L_∞	$L_{2,D}$	$L_{\infty,D}$
20	.28507	.70903	2.88439	3.78547	125.11658
40	.25131	.34881	.52391	2.29930	16.33909
60	.23425	.22288	.31065(-1)	1.65868	14.17259
80	.22425	.30862	4.66287	1.68911	.29991
100	.21903	.26574	1.06674	1.44014	.52915
200	.21504	.24510	.16915	1.35432	7.59734
300	.21498	.24498	.34389	1.35089	1.77678
400	.21497	.24495	.30599	1.35072	1.89423
500	.21497	.24495	.30368	1.35072	1.91675

t	L_{p-1}	L_{p+1}	L_{p+2}
500	.23791	.25044	.25487

Table 6b

Decay parameters B. Perturbed solitary-wave initial profile, $p = 5, \delta = 0.2 \times 10^{-3}, \varepsilon = 0.5 \times 10^{-3}$.

We observe that after an initial transient stage, the $L_q, q = 2, p-1, p, p+1, p+2$ and $L_{2,D}$ rates μ and the associated B's stabilize to constant values. The L_∞ and $L_{\infty,D}$ values also stabilize after a larger time period has elapsed; this probably reflects rougher actual decay of these norms and the extra difficulty generally encountered in pointwise approximation. The eventual rate of decay that emerges from the $L_q, q \leq p+2$ and $L_{2,D}$ columns is clearly $\mu = .78957(-2)$. This is an accurate approximation of $(2\pi)^2\delta = .789568\ldots(-2)$ to five significant digits. The L_∞ and $L_{\infty,D}$ values have three, respectively two, correct digits. It seems safe to conclude then from this experiment that all norms of $u - \overline{u}_0$ decay exponentially in time with decay rate $\mu = (2\pi)^2\delta$ and constants B that depend on the particular norm measured.

In a subsequent experiment, the dissipation constant was doubled to $\delta = .4 \times 10^{-3}$ while keeping all other parameters the same. As a result of the larger value of δ, the decay is faster and the entries stabilized *grosso modo* by $t = 140$. The results are shown (at $t = 140$ only) in Table 7, and confirm the decay rate $\mu = (2\pi)^2\delta$; here the exact value is $(2\pi)^2\delta = .157914(-2)$. We also observe that for all norms the constants B have decreased almost uniformly by about one percent; hence these constants probably depend weakly on δ.

Norm	μ	B
L_2	.15791(-1)	.21269
L_{p-1}	.15792(-1)	.23540
L_p	.15792(-1)	.24237
L_{p+1}	.15792(-1)	.24781
L_{p+2}	.15792(-1)	.25219
L_∞	.15549(-1)	.29101
$L_{2,D}$	.15792(-1)	1.33652
$L_{\infty,D}$	.16900(-1)	2.20768

Table 7
Decay parameters μ and B at $t = 140$.
Perturbed solitary-wave initial profile, $p = 5$, $\delta = 0.4 \times 10^{-3}$, $\varepsilon = 0.5 \times 10^{-3}$.

It should be mentioned that the decay rate $(2\pi)^2\delta$ was confirmed for all the norms and seminorms considered in analogous numerical experiments with a pertrubed solitary-wave initial profile in the case $p = 6$. Finally we experimented with a Gaussian initial profile of the form (4.4) (for which $\overline{u}_0 = .177245$), taking $p = 5$, $\varepsilon = .2 \times 10^{-3}$, $\delta = 10^{-3}$ in (1.3) and integrating up to $t = 80$ by which time the constants μ and B for each norm and seminorm under consideration (including both the L_∞ and $L_{\infty,D}$ entries) had stabilized. The results are shown in Table 8. The computational decay rate μ is again seen to be very close to the value $(2\pi)^2\delta = .394784(-1)$ hypothesized earlier.

Norm	μ	B
L_2	.39478(-1)	.21532
L_{p-1}	.39479(-1)	.23830
L_p	.39479(-1)	.24536
L_{p+1}	.39479(-1)	.25086
L_{p+2}	.39479(-1)	.25530
L_∞	.39496(-1)	.30514
$L_{2,D}$	.39478(-1)	1.35293
$L_{\infty,D}$	.39473(-1)	1.91312

Table 8
Decay parameters μ and B at $t = 80$.
Gaussian initial profile, $p = 5$, $\delta = 10^{-3}$, $\varepsilon = .2 \times 10^{-3}$.

A sample of the simulated temporal evolution of solutions corresponding to the solitary-wave initial condition that yielded the results of Table 6, and to the Gaussian initial condition from which Table 8 was produced, is shown in the sequence of plots of Figures 3 and 4, respectively. In both cases the solutions eventually settle down to profiles resembling sinusoidal waves travelling slowly to the left as they decay to their respective values of $\overline{u}_0$.

An inspection of the first few terms of the series solution of a linear problem associated to (1.2) proves quite illuminating. Defining $\omega(x,t) = u(x,t) - \overline{u}_0$, one expects that since

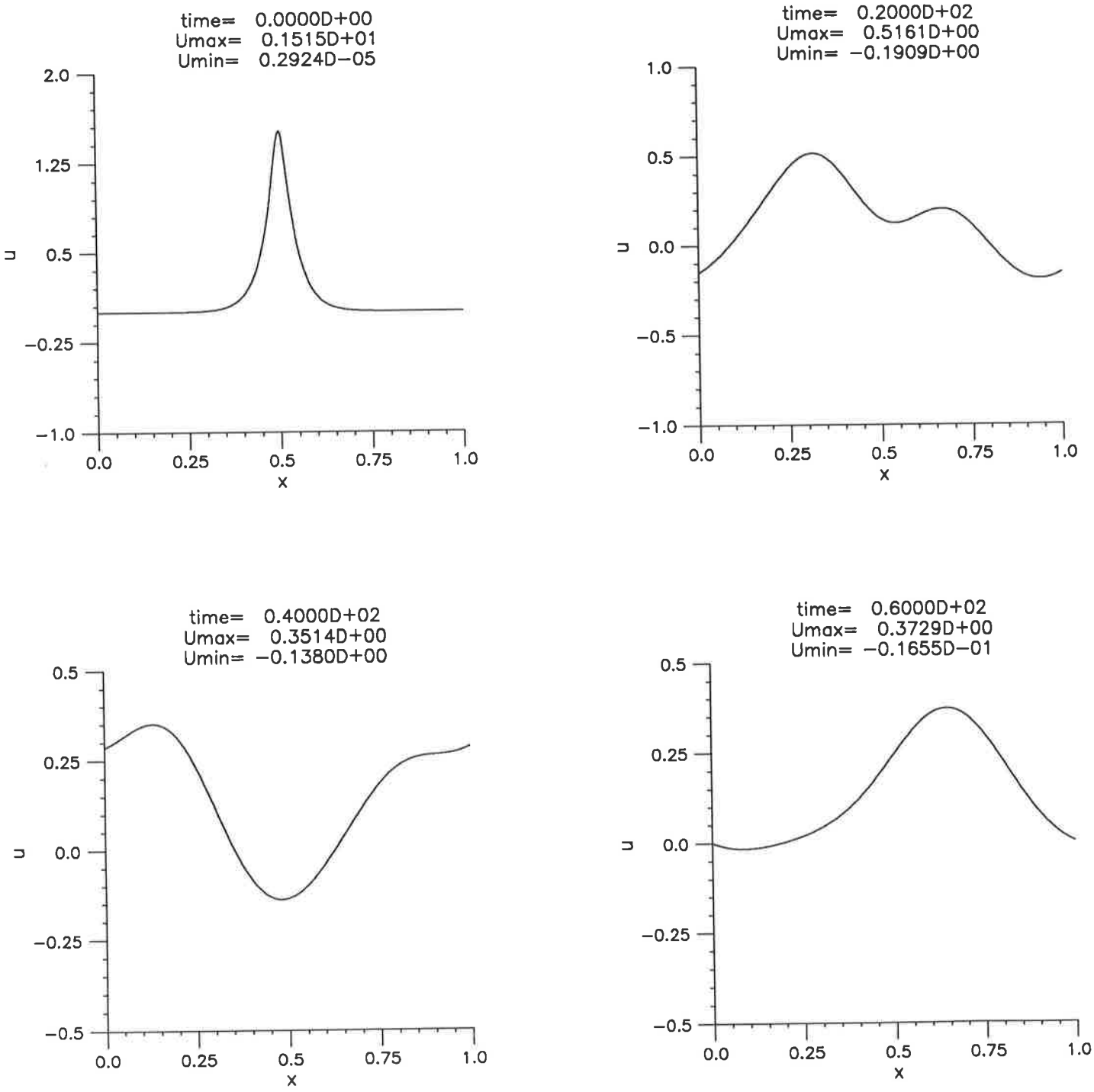

Figure 3a
Long-time decay of solitary-wave initial data. Parameters of Table 6.

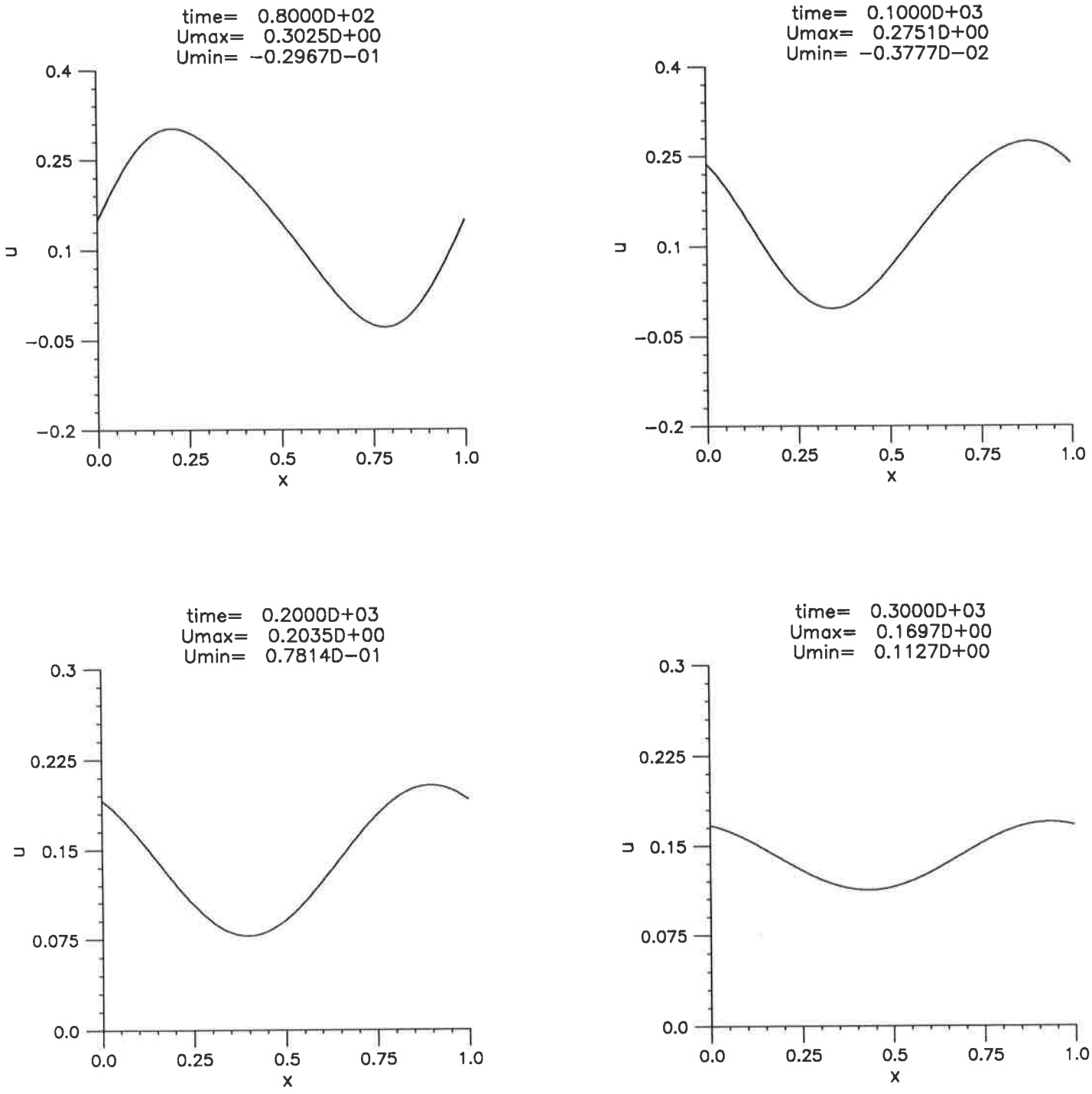

Figure 3b
Long-time decay of solitary-wave initial data, continued.

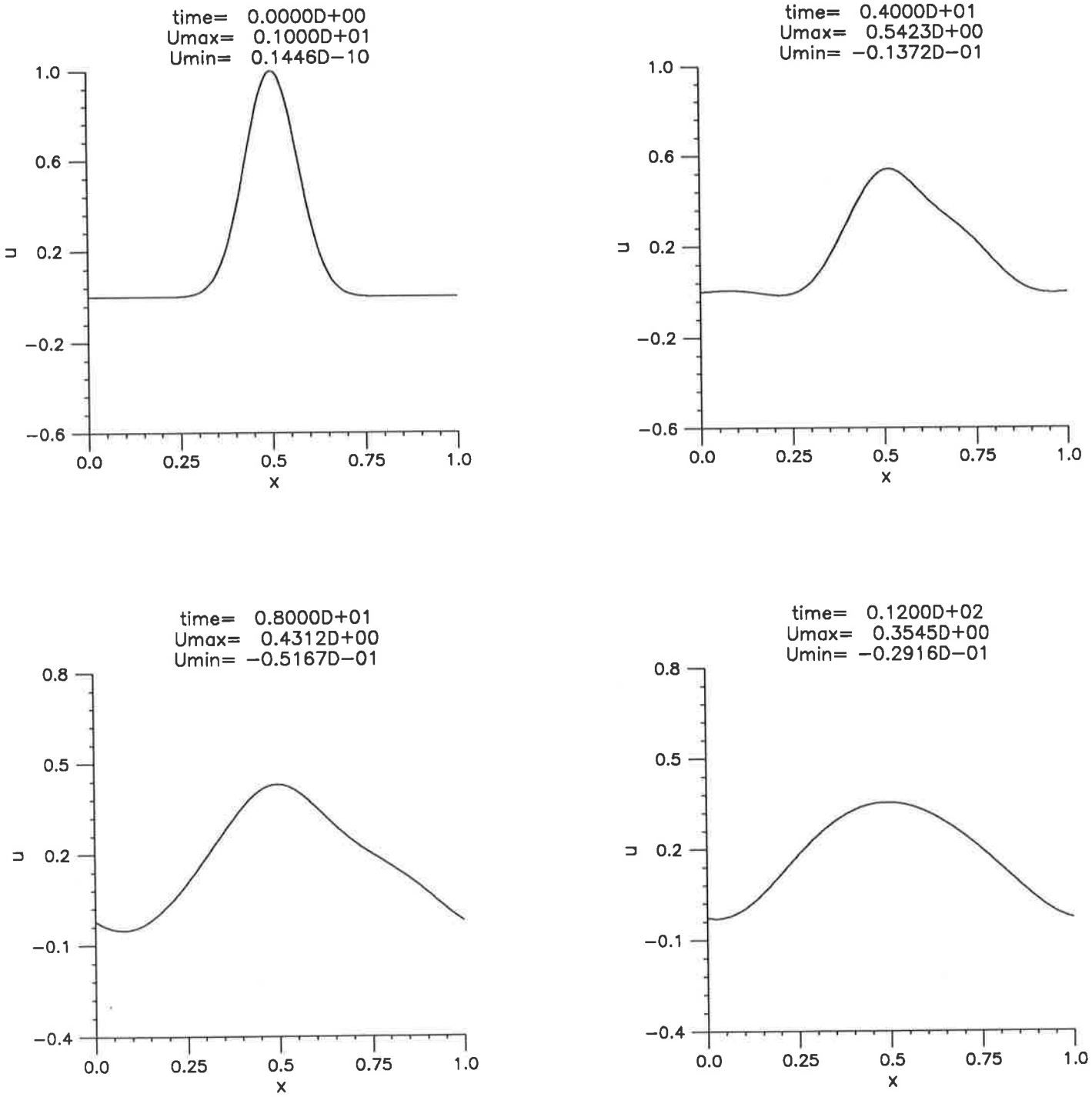

Figure 4a
Long-time decay of Gaussian initial data. Parameters of Table 8.

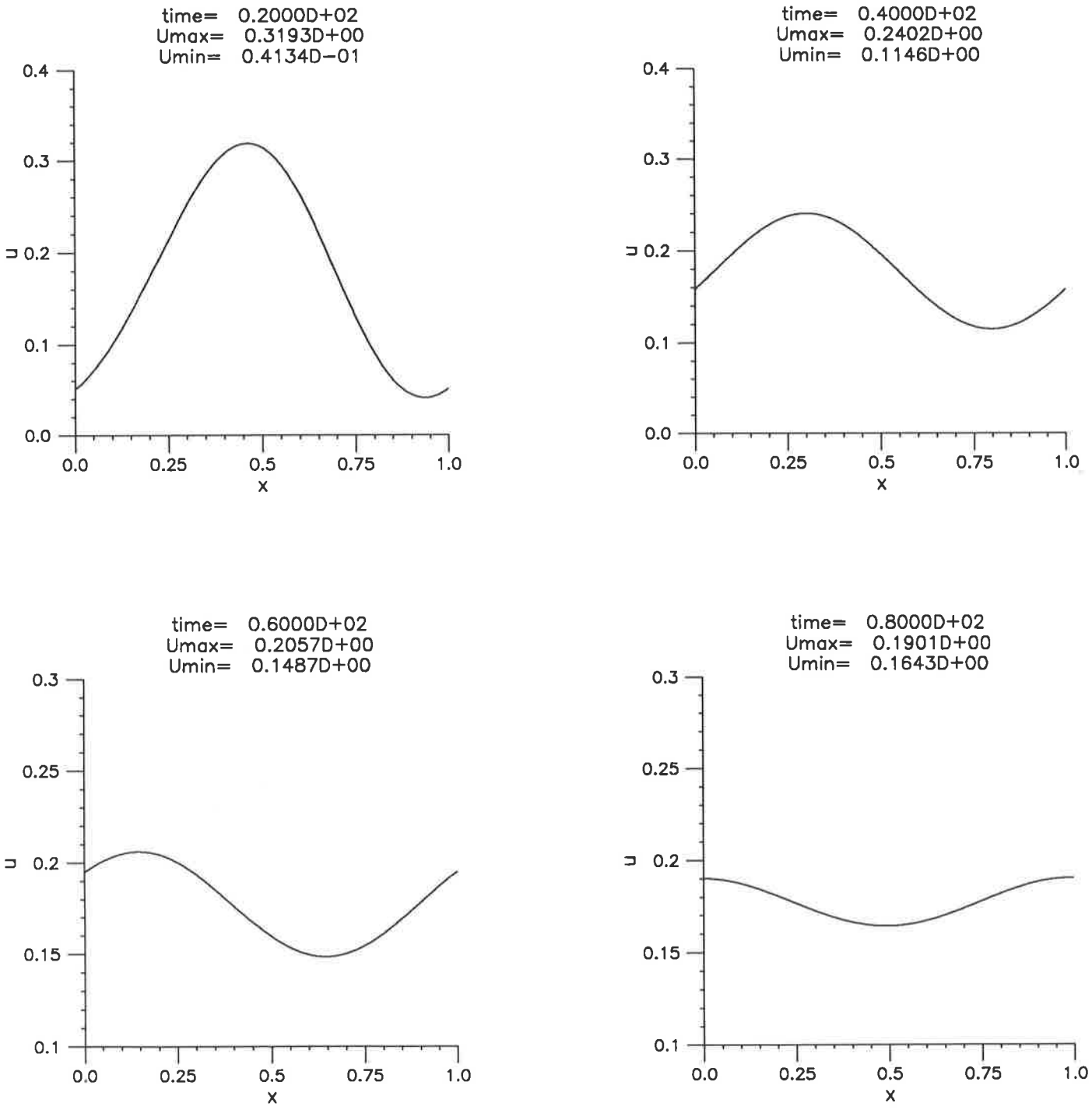

Figure 4b
Long-time decay of Gaussian initial data, continued.

ω tends to zero as t becomes large, for large t the function ω approximately satisfies the linearized dispersive-dissipative equation

$$\omega_t + \eta\omega_x - \delta\omega_{xx} + \varepsilon\omega_{xxx} = 0, \tag{4.7}$$

where $\eta = \overline{u}_0^p$. The solution of (4.7) posed with periodic boundary conditions on $[0,1]$ and with initial condition equal to the 1-periodic function $\omega_0(x) = u_0(x) - \overline{u}_0$ is given by the Fourier series

$$\omega(x,t) = \sum_{n\in\mathbb{Z}} a_n e^{-\delta(2\pi n)^2 t}\, e^{2\pi i n[x-(\eta-\varepsilon(2\pi n)^2)t]},$$

where $a_n = \int_0^1 \omega_0(x)e^{-2\pi i n x}dx$, $n \in \mathbb{Z}$, $a_0 = 0$. Keeping only the lowest frequency, exponentially decaying terms yields the approximation

$$\omega(x,t) \simeq \alpha e^{-(2\pi)^2\delta t}\cos\left\{2\pi[x-(\eta-(2\pi)^2\varepsilon)t]-\xi\right\}, \tag{4.8}$$

where the amplitude coefficient α and the phase shift ξ are constants depending only on the first Fourier components $\int_0^1 \omega_0(x)e^{\pm 2\pi i x}dx$ of ω_0. The relation (4.8) predicts the dominant exponential decay rate $O(e^{-(2\pi)^2\delta t})$ as $t \to \infty$ for solutions of the linear equation; as we have seen this was also observed in the numerical experiments with the nonlinear equation for $u(x,t) - \overline{u}_0$ for very large values of t. It also predicts that the decaying solution asymptotically resembles $\overline{u}_0$ plus a sinusoidal wave profile that, as it decays in amplitude, travels with a speed equal to $\eta - (2\pi)^2\varepsilon = (\overline{u}_0)^p - (2\pi)^2\varepsilon$. This is actually quite close to the value that can be obtained from the output of our numerical experiments. As an example, for the run corresponding to Table 6 and Figure 3, (4.8) predicts a speed equal to -0.01968, which is an excellent approximation to the numerical speed observed in the experiment and computed as follows. Let $X(t)$ denote the point in $[0,1]$ where $u(x,t)$ attains its maximum. Using $t_i = 2(i-2)$, $i \geq 3$ and measuring the speed of the travelling wave at time t_i by the ratio $v_i = (X(t_i) - X(t_{i-1}))/(t_i - t_{i-1})$ (where the variable X is viewed as an element of $\mathbb{R}/Z$ and distances computed accordingly) one obtains Table 9 showing the values of $X(t)$ and v at large values of t_i.

t_i	$X(t_i)$	v_i
200	.8975	-.1853(-1)
300	.9306	-.1971(-1)
400	.9629	-.1967(-1)
500	.9948	-.1962(-1)

Table 9
Long-time speed of the travelling wave, example of Table 6.

Similarly, for the run with a Gaussian initial profile whose evolution was described in Table 8 and Figure 4, (4.8) predicts a speed v equal to $-.00772$. The actual value of v at $t = 80$ was $-.00781$.

Of course the linearized equation provides qualitative information only for very large values of t, when the nonlinear term has ceased to be of any importance. For intermediate values of t, the solution may decay in a complicated way, with energy being exchanged between the lower and the higher modes; in fact, it can be the case that, initially, some of the lower modes will actually increase for a short time due to the nonlinearity. This history of nonlinear decay ought to be reflected, for example, in the constants B in (4.6), which cannot be predicted solely in terms of u_0 as in the linear case. In fact, the weak dependence of B on δ observed in Tables 6 and 7 is probably due to the nonlinearity in the problem. See Amick *et al.* 1989 for commentary on the role of nonlinearity in decaying solutions of (1.2) when the initial-value problem is posed on the entire real line.

Turning now to the short-time decay of solutions of (1.3) and to the formation of the oscillatory tail, we show in Figure 5 the short-time ($0 \leq t \leq 0.2$) evolution, in the case $p = 5$, of an initially unperturbed solitary wave of amplitude $A = 2$, when $\delta = \varepsilon = 0.5 \times 10^{-3}$. The oscillatory tail forms, travels around due to periodicity and starts interacting with the remnant of the main pulse which has not moved appreciably. If the amplitude of the solitary wave is increased, it is observed that the oscillations become more numerous,

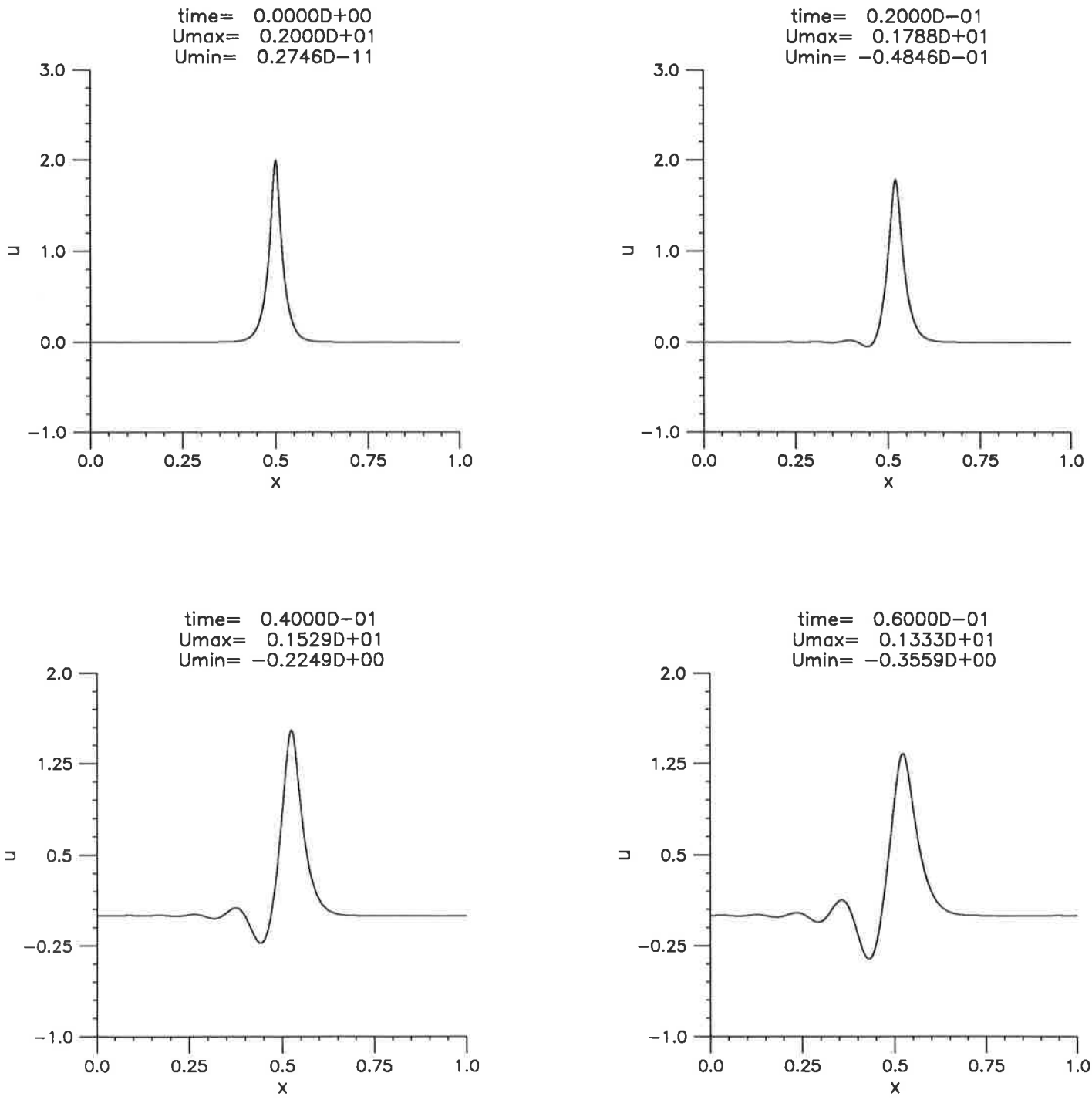

Figure 5a

Initial decay of solitary-wave initial data with $A = 2$, $\varepsilon = 0.5 \times 10^{-3}$, $\delta = 0.5 \times 10^{-3}$.

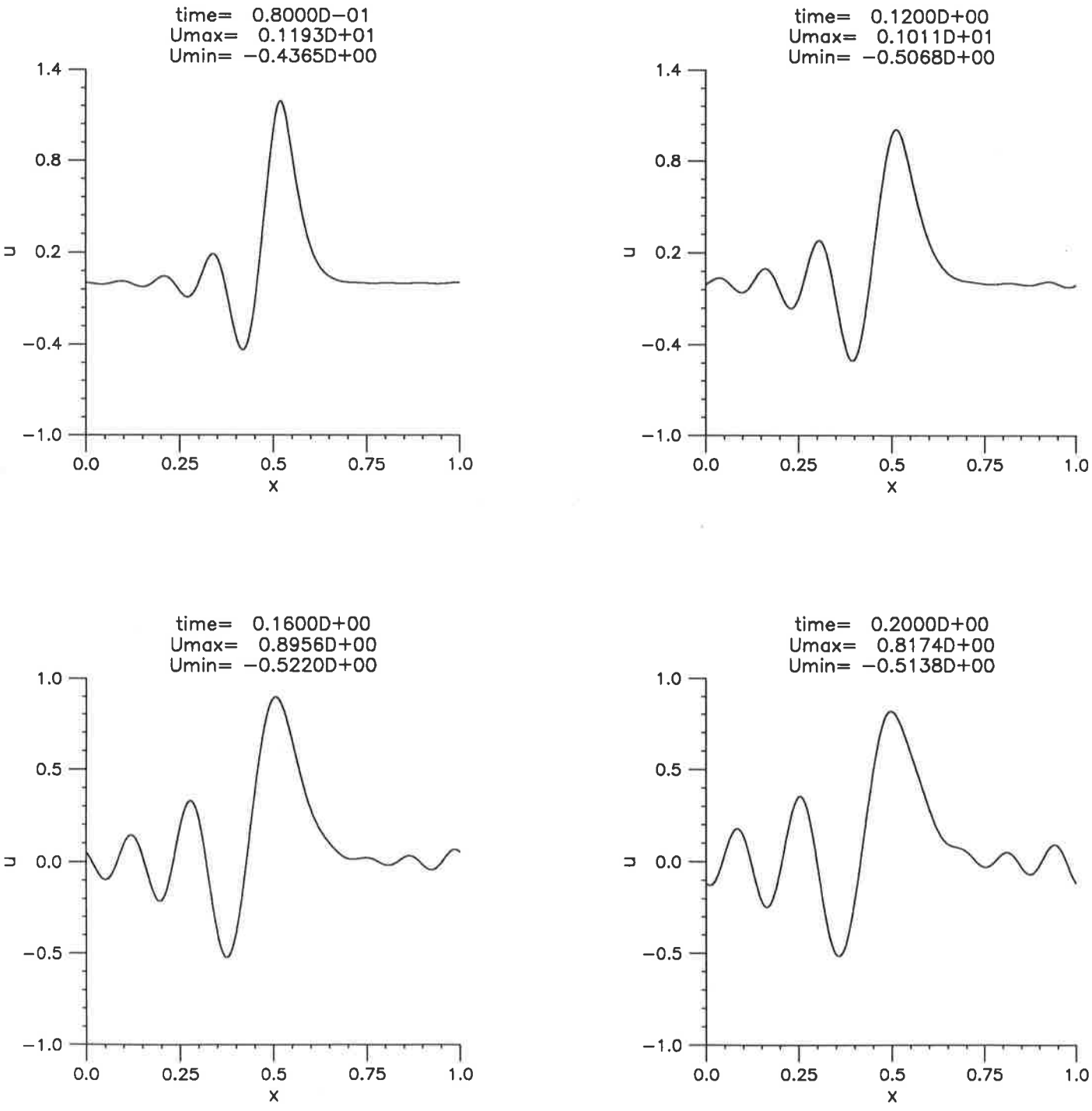

Figure 5b
Initial decay of solitary-wave initial data, continued.

better formed and travel faster. Finally, Figure 6 shows the interesting initial decay of the Gaussian $u_0(x) = e^{-100(x-1/2)^2}$, allowed to evolve under (1.3) with parameters $p = 5$, $\varepsilon = 0.2 \times 10^{-3}$ and $\delta = 0.6 \times 10^{-3}$. The initial profile attempts to resolve itself into solitary-wave pulses that actually grow in amplitude for a while. Had δ been smaller, the leading one would have proceeded to blow-up, as the numerical evidence presented in Section 4a and Bona *et al,* (1994) shows. But, here eventually, the dissipative term dominates and dictates the decay.

5. CONCLUSIONS

The overarching goal of the preceding discussion was to better understand the additional effect of dissipation on solutions of nonlinear, dispersive wave equations. The present study centered around dissipative perturbations of the generalized Korteweg-de Vries equation (1.1a), but it is expected that the information gleaned for this class of equations will provide useful guidance in other, related equations.

It is not surprising that even a small amount of dissipation will substantially alter much of the long-term behavior of solutions. For example, the solitary waves that often appear to play such a fundamental role in the long-term evolution of solutions of initial-value problems like (1.1) for L_2-initial data cease to exist in the face of dissipation. (However, steadily propagating bore-like solutions may well exist in dissipative cases – cf. Bona & Schonbek 1985 and Bona, Rajopadhye & Schonbek 1994.)

The principal focus here has been to comprehend the effect of dissipation on the putative singularity formation observed in (1.1) when $p \geq 4$. The conclusions that form as a result of the information obtained from our numerical experiments are compactly summarized as follows. For suitable s, say $s \geq 2$, let initial data $g \in H^s$ be given. Consider a dissipative perturbation of (1.1a) such as the GKdV-Burgers equation (1.3) or the model (2.14). Let $\nu \geq 0$ connote a parameter like δ in (1.3) or σ in (2.14) that specifies the strength of the perturbation relative to to that of the nonlinear and dispersive terms. Let

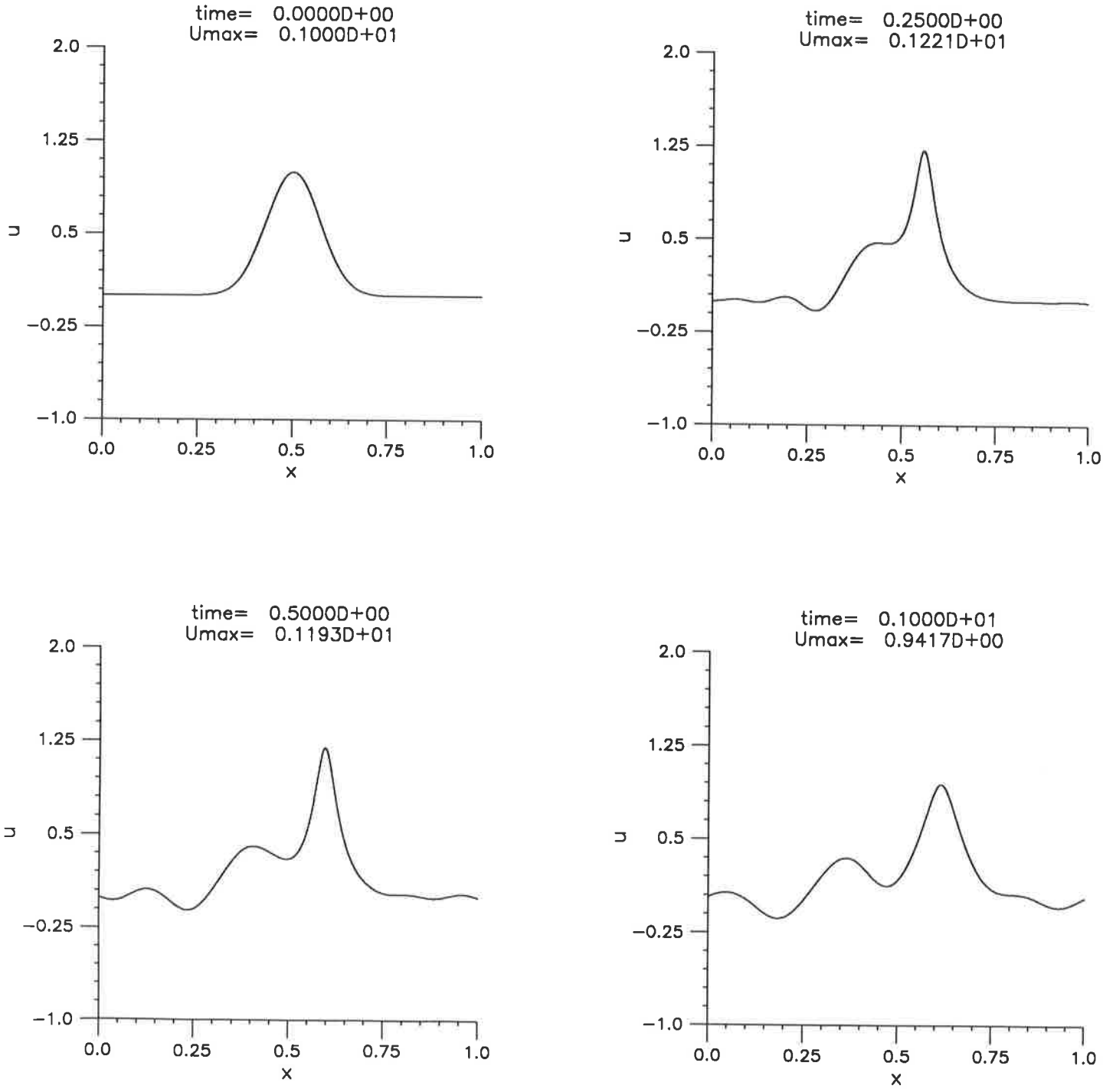

Figure 6
Initial decay of Gaussian initial data $p = 5$, $\varepsilon = 0.2 \times 10^{-3}$, $\delta = 0.6 \times 10^{-3}$.

T_ν denote the maximum existence time for the H^s-solution of the relevant initial-value problem with initial datum g and dissipative parameter ν. That is, for any T in $[0, T_\nu)$, there is a unique H^s-solution defined on $[0, T]$ and T_ν is maximal in this regard. The existence time T_ν is always positive on account of the local well-posedness of the initial-value problem, and either $T_\nu = +\infty$ or the L_∞-norm of the solution becomes unbounded as t approaches T_ν (see Kato 1983, Bona *et al.* 1988). Moreover, simple scaling arguments together with the continuous dependence results make plausible the conjecture that T_ν is an increasing function of ν. The outcome of the numerical experiments reported in Section 4 then indicate the following dichotomy: either

(i) $T_0 = +\infty$, in which case $T_\nu = +\infty$ for all $\nu > 0$,

or

(ii) $T_0 < +\infty$, in which case there exists a critical value ν_c with $0 < \nu_c < +\infty$ such that $T_\nu < +\infty$ for all $\nu < \nu_c$ and $T_\nu = +\infty$ for $\nu \geq \nu_c$.

In the second case, we expect T_ν to be a non-decreasing function of $\nu \in \mathbb{R}^+$ with values in the extended positive real numbers $\mathbb{R}^+ \cup \{+\infty\}$, and continuous except perhaps at ν_c where there may be a jump discontinuity.

If $T_0 < +\infty$, then our experiments also indicate that the structure through which singularity formation occurs varies only slightly with ν until ν_c is reached. However, the two different dissipative mechanisms considered showed a different dependence upon the parameter p.

It would be interesting and relevant to important modelling situations to broaden the range of dissipative mechanisms considered. A natural class of local dissipative terms that deserves consideration in conjunction with the GKdV equation is $(-1)^j \partial_x^{2j}$, $j = 2, 3, \ldots$. It is straightforward to determine that the initial-value problem for the GKdV equation with the term $\nu(-1)^k \partial_x^{2k} u$, $\nu > 0$ appended is globally well posed for arbitrary sized initial data if $p < 4k - 2$. It could be instructive to learn what happens if $\nu > 0$, $k \geq 2$ and $p > 4k - 2$. The case $k = 2$ may already be quite different from the cases $k = 0$ and $k = 1$

examined here because for $k \geq 2$ the critical value of the parameter p in the nonlinearity is determined solely by the dissipative term rather than the dispersive term. Non-local dissipative processes also arise as models in practically interesting situations. Broadening still further the range of inquiry might lead to the GKdV equation with dissipative perturbation $\nu M_\alpha u$, where $\hat{M_\alpha v}(\xi) = |\xi|^\alpha \hat{v}(\xi)$ is a homogeneous Fourier multiplier operator. The decay of solutions of the initial-value problem

$$u_t + u^p u_x + u_{xxx} + \nu M_\alpha u = 0,$$

$$u(x,0) = g(x)$$

has been studied when g is suitably small (see Dix 1992, Bona, Promislow & Wayne 1994, Bona & Demengel 1994). However, the situation that obtains for larger initial values has thus far resisted analysis, and careful numerical simulation would be welcome.

Acknowledgements

The authors gratefully acknowledge support and hospitality from the Institute of Applied and Computational Mathematics at the Research Center of Crete, FORTH, and the Mathematics Department at Penn State. The collaboration was materially aided by a joint travel grant from the National Science Foundation, USA, and the General Secretariat of Research & Technology, Greece. JLB and OAK also acknowledge general support from the National Science Foundation and the University of Tennessee Science Alliance.

References

Albert, J.P. & Bona, J.L. 1991 Comparisons between model equations for long waves. *J. Nonlinear Sci.* **1**, 345–374.

Albert, J.P., Bona, J.L. & Felland, F. 1988 A criterion for the formation of singularities for the generalized Korteweg-de Vries equation. *Mat. Aplic. e Comp.* **7**, 3–11.

Amick, C.J., Bona, J.L. & Schonbek, M.E. 1989 Decay of solutions of some nonlinear wave equations. *J. Diff'l. Eqns.* **81**, 1–49.

Baker, G., Dougalis, V.A. & Karakashian, O.A. 1983 Convergence of Galerkin approximations for the Korteweg-de Vries equation. *Math. Comp.* **40**, 419–433.

Benjamin, T.B. 1974 Lectures on nonlinear wave motion. In *Lectures in Applied Mathematics* **15**, pp. 3–47, (A. Newell, ed.) American Math. Soc.: Providence.

Benjamin, T.B., Bona, J.L. & Mahony, J.J. 1972 Model equations for long waves in nonlinear, dispersive media. *Philos. Trans. Royal Soc. London A* **272**, 47–78.

Biler, P. 1984 Large-time behaviour of periodic solutions to dissipative equations of Korteweg-de Vries-Burgers type. *Bull. Polish Acad. Sci. Math.* **32**, 401–405.

Bona, J.L. 1981 Convergence of periodic wave trains in the limit of large wavelength. *Appl. Sci. Res.* **37**, 21–30.

Bona, J.L. & Demengel, F. 1994 Non-local dissipation and the decay of nonlinear dispersive waves. To appear.

Bona, J.L., Dougalis, V.A. & Karakashian, O.A. 1986 Fully discrete Galerkin methods for the Korteweg-de Vries equation. *Comp. & Maths. with Applics.* **12A**, 859–884.

Bona, J.L., Dougalis, V.A., Karakashian, O.A. & McKinney, W.R. 1992 Computations of blow-up and decay for periodic solutions of the generalized Korteweg-de Vries equation. *Appl. Numerical Math.* **10**, 335–355.

Bona, J.L., Dougalis, V.A., Karakashian, O.A. & McKinney, W.R. 1994 Conservative, high-order numerical schemes for the generalized Korteweg-de Vries equation. To appear in *Philos. Trans. Royal Soc. London A.*

Bona, J.L. & Luo, L. 1993 Decay of solutions to nonlinear, dispersive wave equations. *Differential & Int. Equations* **6**, 961–980.

Bona, J.L., Pritchard, W.G. & Scott, L.R. 1981 An evaluation of a model equation for water waves. *Philos. Trans. Royal Soc. London A* **302**, 457–510.

Bona, J.L., Promislow, K. & Wayne, G. 1994 On the asymptotic behavior of solutions to nonlinear, dispersive, dissipative wave equations. To appear in *J. Math. & Comp.*

Bona, J.L., Rajopadhye, S. & Schonbek, M.E. 1994 Models for propagation of bores I. Two-dimensional theory. *Differential & Int. Equations* **7**, 699–734.

Bona, J.L. & Schonbek, M.E. 1985 Travelling-wave solutions to the Korteweg-de Vries-Burgers equation. *Proc. Royal Soc. Edinburgh* **101A**, 207–226.

Bona, J.L. & Sciálom, M. 1993 The effect of change in the nonlinearity and the dispersion relation on model equations for long waves. To appear in *Canadian J. Appl. Math.*

Bona, J.L. & Smith, R. 1975 The initial-value problem for the Korteweg-de Vries equation. *Philos. Trans. Royal Soc. London A* **278**, 555–604.

Bona, J.L., Souganidis, P.E. & Strauss, W.A. 1987 Stability and instability of solitary waves of KdV type. *Proc. Royal Soc. London A* **411**, 395–412.

Bourgain, J. 1993 Fourier transform restriction phenomena for certain lattice subsets

and applications to non-linear evolution equations. Preprint.

Dix, D.B. 1992 The dissipation of nonlinear dispersive waves: The case of asymptotically weak nonlinearity. *Comm. P.D.E.* **17**, 1665–1693.

Foias, C. & Saut, J.-C. 1984 Asymptotic behavior, as $t \to +\infty$ of solutions of Navier-Stokes equations and nonlinear spectral manifolds. *Indiana Univ. Math. J.* **33**, 459–477.

Grad, H. & Hu, P.N. 1967 Unified shock profile in a plasma. *Phys. Fluids* **10**, 2596–2602.

Jeffrey, A. & Kakutani, T. 1972 Weak nonlinear dispersive waves: a discussion centered around the Korteweg-de Vries equations. *SIAM Rev.* **14**, 582–643.

Johnson, R.S. 1970 A nonlinear equation incorporating damping and dispersion. *J. Fluid Mech.* **42**, 42–60.

Karakashian, O.A. & McKinney, W.R. 1990 On optimal high order in time approximations for the Korteweg-de Vries equation. *Math. Comp.* **55**, 473–496.

Karakashian, O.A. & McKinney, W.R. 1994 On the approximation of solutions of the generalized Korteweg-de Vries-Burgers equation. Submitted.

Kato, T. 1975 Quasilinear equations of evolution with applications to partial differential equations. *Lecture Notes in Math.* **448**, 25–70.

Kato, T. 1979 On the Korteweg-de Vries equation. *Manuscripta Math.* **28**, 89–99.

Kato, T. 1983 On the Cauchy problem for the (generalized) Korteweg-de Vries equation. *Studies in Appl. Math., Advances in Mathematics Supplementary Studies*, Academic Press: New York, **8**, 93–130.

Pego, R.L. 1985 Remarks on the stability of shock profiles for conservation laws with dissipation. *Trans. American Math. Soc.* **291**, 353–361.

Pego, R.L. & Weinstein, M.I. 1992 Eigenvalues, and instabilities of solitary waves. *Philos. Trans. Royal Soc. London A* **340**, 47–94.

Schechter, E. 1978 Well-behaved evolutions and the Trotter product formulas. *Ph.D. Thesis*, University of Chicago.

Scott, A.C., Chu, F.Y.F. & McLaughlin, D.W. 1973 The soliton: A new concept in applied science. *Proc. IEEE* **61**, 1443–1483.

Strauss, W.A. 1974 Dispersion of low-energy waves for two conservative equations. *Arch. Rational Mech. Anal.* **55**, 86–92.

Zhang, B.-Y. 1993 Remarks on Cauchy problem of the Korteweg-de Vries equation on a periodic domain. Preprint.

Zhang, L. 1994 Decay of solutions of generalized Benjamin-Bona-Mahony equations. To appear.